Since January 2020 Elsevier has created a COVID-19 resource centre with free information in English and Mandarin on the novel coronavirus COVID-19. The COVID-19 resource centre is hosted on Elsevier Connect, the company's public news and information website.

METABOLISM CLINICAL AND EXPERIMENTAL 65 (2016) 1247–1258

Available online at www.sciencedirect.com

Metabolism

www.metabolismjournal.com

Basic Science

Apolipoprotein D deficiency is associated to high bone turnover, low bone mass and impaired osteoblastic function in aged female mice

Corine Martineau[a,*,1], Ouafa Najyb[b], Céline Signor[a], Éric Rassart[b], Robert Moreau[a,2]

[a] Laboratoire du Métabolisme Osseux, Centre BioMed, Département des Sciences Biologiques, Université du Québec à Montréal, Montréal, Québec, Canada

[b] Laboratoire de Biologie Moléculaire, Centre BioMed, Département des Sciences Biologiques, Université du Québec à Montréal, Montréal, Québec, Canada

ARTICLE INFO

Article history:
Received 3 November 2015
Accepted 10 May 2016

Keywords:
Apolipoprotein D
Osteoblast
Proliferation
Differentiation
Low bone mass

ABSTRACT

Background. Apolipoprotein D (ApoD) is a member of the lipocalin family known to transport small hydrophobic ligands. A major site of *ApoD* expression in mice is the central nervous system where evidence suggests that it plays a protective role. Gene expression of *ApoD* was reported in bone-forming osteoblasts but its impact on bone metabolism remains undocumented.

Methods. We compared basic bone parameters of *ApoD*$^{-/-}$ (null) and transgenic (tg) mice to wild-type (wt) littermates through microCT and histochemistry, as well as *ApoD* expression and secretion in osteoblasts under various culture conditions through real-time PCR and immunoblotting.

Results. *ApoD*-null females displayed progressive bone loss with aging, resulting in a 50% reduction in trabecular bone volume and a 23% reduction in cortical bone volume by 9 months of age. Only cortical bone volume was significantly reduced in *ApoD*-null males by an average of 24%. Histochemistry indicated significantly higher osteoblast surface and number of osteoclasts in femora from *ApoD*-null females. *ApoD* gene expression was confirmed in primary cultures of bone marrow mesenchymal cells (MSC), with higher expression levels in MSC from females compared to males. *ApoD*-null MSC exhibited impaired proliferation and differentiation potentials. Moreover, exogenous ApoD partially rescued the osteogenic potential of null MSC, which were shown to readily uptake the protein from media. *ApoD* expression was upregulated under low proliferation conditions, by contact inhibition and osteoblastic differentiation in MC3T3-E1 osteoblast-like cells.

Conclusion. Our results indicate that ApoD influences bone metabolism in mice in a gender-specific manner, potentially through an auto-/paracrine pathway.

* *Corresponding author at:* CP 8888, Succ Centre-Ville, Montréal, Québec, Canada H3C 3P8.
E-mail addresses: cmartineau@shriners.mcgill.ca, martineau.corine@courrier.uqam.ca (C. Martineau).
[1] Present address: Genetic Unit, Shriners Hospitals for Children — Canada, Montréal, Québec, Canada.
[2] Author deceased as of July 23rd 2015.

http://dx.doi.org/10.1016/j.metabol.2016.05.007
0026-0495/

1. Introduction

Bone is a dynamic tissue that undergoes continuous remodeling through coordinated processes of bone resorption and formation. The balance between both processes preserves bone tissue integrity and mineral homeostasis of the organism [1]. Osteoclasts and osteoblasts are specialized cells which respectively break down old bone tissue and promote the formation of new bone matrix. Osteoblasts, under the control of specific transcription factors, sequentially differentiate from bone marrow mesenchymal stem cells (MSC) into proliferating preosteoblasts, bone matrix-producing osteoblasts, and eventually into osteocytes embedded within the bone matrix [2]. Differentiated osteoblasts synthesize and secrete type I collagen, the main bone matrix protein, and regulate bone mineralization through expression of alkaline phosphatase and osteocalcin. In addition, these cells orchestrate bone remodeling by regulating the activation and differentiation of bone-resorbing osteoclasts from the monocyte/macrophage lineage [1]. Any imbalance between resorptive and formative functions of these cell populations may lead to excessive bone resorption or inadequate formation, resulting in loss of bone density, lower bone mass and increased risk of bone fractures [3] as observed in osteoporosis.

Apolipoprotein D (ApoD) is a 29-kDa glycoprotein first isolated from high density lipoprotein (HDL) plasma fractions [4]. Unlike other apolipoproteins, which are essentially produced in liver and intestine, ApoD is mainly expressed in the central nervous system (CNS) [5]. Molecular cloning and structural analyses revealed that this protein is part of the lipocalin superfamily [6]. Lipocalins share a conserved 8 beta barrel strand structure, forming a pocket with high affinity for small hydrophobic ligands. Several molecules were identified as potential ligands for ApoD: arachidonic acid, progesterone, pregnenolone, bilirubin, cholesterol and E-3-methyl-2-hexenoic acid (reviewed in Ref. [7]). Binding studies revealed that ApoD is able to discriminate between closely related compounds [8]. Due to this apparent heterogeneity, a role as a 'multi-ligand:multi-function' protein has been proposed [7]. *ApoD* expression is induced by growth arrest [9,10], inflammation and oxidative stress [11,12]. The CNS was shown to be the major site of *ApoD* expression in mice and rats [5] and therefore, its physiological functions have mainly been studied in the nervous tissue. In rats, ApoD levels increase considerably in peripheral nervous tissue after experimental nerve injury [13–15]. In humans, ApoD expression is induced by several neurodegenerative and psychiatric disorders (for a review [16,17]). Thus, there is accumulating evidence suggesting that ApoD plays a protective role in the CNS. Of interest, higher *ApoD* expression levels are measured in women; moreover, these levels increase with age in women but not in men [18]. The protein is also overexpressed in several types of cancer [19,20], in lipid metabolism disorders such as Tangier disease [21], abetalipoproteinemia [22,23], LCAT deficiency [24], hypertriglyceridemia at birth [25], and in pathological conditions leading to lipid accumulation such as non-insulin dependent diabetes mellitus (NIDDM) [26,27].

Microarray analyses suggest that the basal *ApoD* gene expression in human MSC is increased during osteogenic differentiation [28]. Similar observations were reported in the murine MSC-like cell line C3H10 [29] and in mouse primary osteoblasts [30]. Although limited in number, these studies suggest a potentially significant involvement of ApoD in bone metabolism. The present work explored the regulation of ApoD expression in osteoblasts under various culture conditions, and tried to determine the extent of its contribution to bone metabolism using *ApoD*-deficient (null) and human *ApoD* transgenic (tg) mouse models.

2. Materials and methods

2.1. Animals and Plasma Analysis

ApoD-null mice were generated on a C57Bl/6J background by inserting a targeting vector with the neomycin phosphotransferase (Neo) gene interrupting exon 6 of the *ApoD* gene (for the complete protocol, see Ref. [12]). Heterozygous females were crossbred with null males: the resulting progeny were analyzed. The human *ApoD* transgenic (h*ApoD*-tg) mice were generated as described in Ref. [12]. Briefly, these mice carry a construct (~4.5 kb) containing the promoter, the first exon, the first intron and the 5′ noncoding region of the second exon of the human Thy-1 gene (generous gift from J. Silver, New York University Medical Center). This fragment was fused to the h*ApoD* coding sequence followed by the bovine growth hormone (BGH) polyadenylation signal. Mice were backcrossed with C57BL6 mice for at least 10 generations.

This study was conducted according to protocols approved by the Institutional Animal Care and Use Committee (IACUC, #706) of Université du Québec à Montréal. No significant difference was noted in body weight for either mouse strain at all ages used in this study (Table 1). Following isoflurane general anesthesia, whole blood was harvested from 9-month-old mice through cardiac punctures and collected in 3 mL heparinated tubes (68 USP, BD Bioscience, Mississauga, ON, Canada) and mice were sacrificed by cervical dislocation. Plasma was

Table 1 – Weight of 3 to 9-month-old wt, *ApoD*-null and h*ApoD*-tg male and female mice.

Gender	Male			Female		
Genotype	wt	null	tg	wt	null	tg
3 months	24.4 ± 1.0	26.6 ± 1.0	23.5 ± 1.1	19.7 ± 0.7	20.4 ± 0.6	21.0 ± 0.4
6 months	35.5 ± 2.3	34.4 ± 2.5	40.4 ± 3.5	26.4 ± 1.0	28.7 ± 0.9	29.0 ± 1.2
9 months	42.5 ± 1.5	40.8 ± 1.7	42.4 ± 2.4	29.8 ± 1.8	32.2 ± 1.7	30.7 ± 2.0

Body weight (g) was determined in 6–10 mice per group. No significant difference was observed between age- and gender-matched wt, null and tg mice, 2-way ANOVA followed by a Bonferroni post-hoc test.

obtained by centrifugation at 2000*g* for 25 min at 4 °C and stored at −80 °C until analyses. Alkaline phosphatase, calcium and phosphate were evaluated with colorimetric QuantiChrom assays (BioAssay Systems, Hayward, CA, USA).

2.2. Documentation of Bone Architecture

Following euthanasia, femora from 3-, 6- and 9-month-old mice were harvested and fixed in 4% paraformaldehyde-phosphate buffered saline (PF) at 4 °C for 16–20 h. MicroCT analyses were performed using a Skyscan 1172c X-ray computed microtomograph (Skyscan, Kontich, Belgium) equipped with an X-ray tube working at 70 kV/100 μA. Femora of wt, *ApoD*-null and h*ApoD*-tg mice were scanned at a 5 μm pixel size, a 180° rotation with a 0.5° rotation increment using a 0.5 mm aluminum filter. Stacks of 2D X-ray shadow projections were reconstructed with a 0 to 0.09 dynamic range to obtain cross-sectional images using NRecon (Skyscan), and subjected to morphometric analyses using CTAn (Skyscan). Trabecular parameters were measured at the metaphysis (400 slices – 2 mm – were selected 100 slices below the growth plate); the cortical region consisted of 100 slices – 0.5 mm – selected 600 slices below the growth plate reference point. The parameters measured included trabecular bone volume (bone volume/tissue volume (BV/TV)), trabecular thickness (Tb.Th), number of trabeculae (Tb.N), trabecular separation (Tb.Sp), as well as cortical bone volume (Ct.BV), cortical thickness (Ct.Th) and cortical diameter (Ct.Dm). Three-dimensional renderings were generated from these volumes of interest using CTvol (Skyscan).

Paraformaldehyde (PF)-fixed undecalcified bones were embedded in low-temperature polymerizing polymethylmethacrylate (PMMA) as previously described [31], sectioned at 6 μm with a Thermofisher rotary HM 360 microtome and used for Von Kossa, alkaline phosphatase (ALP) (Millipore, Billerica, MA, USA) and tartrate resistant acid phosphatase (TRAP) (K Assay, Dako, Burlington, ON, Canada) histochemical stainings. Von Kossa (bone area per tissue area — B.Ar/T.Ar), ALP (osteoblast surface — Ob.S) or TRAP-stained (number of osteoclasts — Oc.N/mm) bone sections were visualized with an inverted phase contrast microscope (TE-300, Nikon, Mississauga, ON, Canada) and analyzed with ImageJ.

2.3. Cell Culture

Long bones from 2 to 4 month-old female mice hind limbs were harvested and sterilized in phosphate-buffered saline (PBS) containing 200 U/mL penicillin-200 μg/mL streptomycin and 1% FungiZone (all from Invitrogen). Epiphyses were cut off under sterile hood, marrow was flushed out, suspended in αMEM supplemented with 100 U/mL penicillin, 100 μg/mL streptomycin, 2 mmol/L L-glutamine, 10% FBS, and 25 μg/mL L-ascorbic acid (Sigma) and plated in 100 mm culture dish (Sarstedt, Montréal, QC, Canada). Bones from 1 mouse were used per dish, unless specified otherwise. Cells were left to adhere for 7 days, and then thoroughly washed with PBS to eliminate non adherent cells. Adherent cells were left to reach confluence prior to harvest and experimentation. For primary cultures of osteoblasts, bone fragments from femora and tibiae were subjected to three consecutive digestions with collagenase IA (Sigma); fragments were plated with αMEM medium containing 1% FungiZone (Invitrogen) and 10% FBS in 100 mm dishes (Sarstedt) until cell outgrowth to confluent monolayers.

MC3T3-E1 osteoblast-like cells derived from mouse calvaria and constitute a well-known *in vitro* model for studying osteoblast function [32]. MC3T3 cells (American Type Culture Collection, ATCC; Rockville, MD, USA) were maintained in alpha-modified minimum essential medium (αMEM; Sigma, Oakville, ON, Canada) containing 10% fetal bovine serum (FBS; NorthBio, Toronto, ON, Canada), 2 mmol/L L-glutamine (Invitrogen, Burlington, ON, Canada), 100 U/mL penicillin (Invitrogen), and 100 μg/mL streptomycin (Invitrogen), and subcultured every 7 days with 0.05% trypsin-0.02% EDTA solution (Invitrogen).

2.4. MTT Assay, Cell Cycle Analysis and BrdU Incorporation

For proliferation assays, primary cells were plated in 96-well plates at 20,000 cells per cm^2 and cell metabolic activity was evaluated 24 h later (day 0) as well as on days 1, 3, 6, 10 and 14, through tetrazolium microtiter (MTT) assay (Sigma). For analyses of DNA synthesis, cell cycle and gene expression, MC3T3 cells were cultured in medium containing 10% FBS (control) or serum-starved for 48 h (low proliferation condition), or cultured in medium containing 10% FBS until monolayers reached sub-confluence (70%), 100% confluence, and 3 days after reaching confluence (post-confluence). For evaluation of DNA synthesis, cells were seeded in 96-well plates (Sarstedt) at 2500 cells/cm^2 and cultured under the proliferation or confluence conditions described above. DNA synthesis was determined by BrdU incorporation and detected using an ELISA kit (Roche Diagnostics, Laval, QC, Canada) following manufacturer recommendations. Briefly, cells were incubated with BrdU for the last 2 h of treatment, then fixed and treated with a nuclease solution. Incorporated BrdU was detected with anti-BrdU-POD for 30 min and revealed with a peroxidase substrate. For cell cycle analysis, cells cultured in parallel under the same conditions were stained with propidium iodide (PI) and analyzed by flow cytometry (FACScan, Becton Dickinson) using FlowJo software (version 8.7.3).

2.5. Osteogenic Conditions, hApoD Treatment and hApoD Uptake

To verify the short term effect on *Opg*, *Rankl* and *Sod1* expression, wt and null MSC were treated with 250 ng/mL of hApoD for 24 h. The impact of hApoD on osteogenic differentiation was compared to that of basal MEM medium and to regular osteogenic medium. Briefly, confluent cells were treated for 21 days (MC3T3-E1 cells) or 14 days (wt and null MSC) with or without 250 ng/mL hApoD or 50 μg/mL ascorbic acid (Sigma) and 5 mmol/L glycerol-2-phosphate (Sigma); media were changed 3 times a week. The effectiveness of treatments was monitored through alkaline phosphatase (ALP) activity *versus* cultures in basal medium, with cytochemical staining (Millipore, Billerica, MA, USA) and *p*-nitrophenylphosphate conversion to *p*-nitrophenolate (as described in Ref. [33]). In parallel, marrow-derived primary cells were cultured onto glass slides and exposed to 250 ng/mL FITC-labeled hApoD for 24 h. Cells were then rinsed with PBS and fixed with 10% formalin, then permeabilized with 0.1% triton X-100 (*w/v*) and stained with PI. hApoD and PI

fluorescence were visualized with an inverted phase contrast microscope (TE-300; Nikon, Mississauga, Ontario, Canada) at a 40× magnification.

2.6. PCR Amplification

Total RNA was extracted using TriZol (Invitrogen) according to the manufacturer's instructions. Reverse transcription (RT) reactions were carried out with Omniscript RT kit (Qiagen, Mississauga, ON, Canada) using random hexamers (Invitrogen). PCR amplifications for semi-quantitative analysis were conducted with *Taq* PCR core kit (Qiagen) using specific primer sets for murine *ApoD* (F: 5′-CCACCGGCACCCTACTGGATC-3′, R: 5′-CGGGCAGTTCGCTTGATCTGT-3′) and human *ApoD* (F: 5′-TTA ACCTCACAGAGCCTGCC-3′, R: 5′-GAGTCCACTGTTTCTGGAG GG-3′); *Gapdh* (F: 5′-AGAACATCATCCCTGCATCC-3′, R: 5′-AGTT GCTGTTGACGTCGC-3′) was used as a reference gene for normalization. Amplifications were carried out for 40 cycles of 1 min at 94 °C, 30 s at 58 °C and 1 min at 72 °C. PCR products were resolved in 2% agarose gel and visualized under UV with Redsafe (FroggaBio, North York, ON, Canada) staining. Real-time PCR analysis for mouse *ApoD*, *Opg*, *Rankl* and *Sod1* was performed using the iCycler IQ detection system (Bio-Rad, Hercules, CA, USA) and SYBR Green I (Bio-Rad) as a double-strand DNA-specific binding dye, using *β-microglobulin* (*B2m*) as a reference gene (F: 5′-TACTCAGCCACCCACCGGCCG-3′, R: 5′-GCTCGGCCATACTGGCATGCT-3′) and the following sets of specific primers: *Opg* (F: 5′-GTGTGGAATAGATGTCACCCTGT-3′, R: 5′-CTTGTGAGCTGTGTCTCCGT-3′), *Rankl* (F: 5′-CCCATCG GGTTCCCATAAAGT-3′, R: 5′-AGCAAATGTTGGCGTACAGG-3′) and *Sod1* (F: 5′-CACTTCGAGCAGAAGGCAAG-3′, R: 5′-CCCCATA CTGATGGACGTGG-3′). Each sample was run in triplicate, and fluorescence data were collected at the end of each cycle. Each run ended with a melting curve to ensure amplification specificity (from 60 to 95 °C at a 0.5 °C/10 s rate). Expression levels were calculated using the comparative CT method [i.e., $1/(\Delta\Delta CT)$, where ΔCT is the difference between CT target and CT reference] after normalization to *B2m* expression level, and relative fluorescence units (RFU) were analyzed using optical system software Version 3.1 (Bio-Rad).

2.7. Western Blot

MC3T3-E1 cells were grown to confluence in 12-well plates (Sarstedt), cultured in control or osteogenic medium for 21 days and analyzed for ApoD expression and secretion on days 0, 7, 14 and 21. Twenty four h prior to protein or RNA extraction, medium was changed for FBS-free MEM which was collected at time of extraction to recuperate secreted ApoD. Cellular proteins were extracted in lysis buffer for immunoblotting, as RNA was retrieved by TriZol (Invitrogen) for PCR analysis. For protein secretion, 40 μL of media was loaded per well; for protein expression, 10 μg of cell extract was loaded per well. All samples were mixed with 5× denaturing loading buffer and resolved on a 12% SDS-PAGE (Bio-Rad Laboratories, Mississauga, Canada). Gels were transferred onto PVDF membranes and immunoblotted with a mouse-specific goat anti-ApoD (1:1000, sc34760, Santa-Cruz sc34760 biotechnology, Dallas, TX, USA), followed by an anti-goat secondary antibody (1:10,000, Santa Cruz) coupled to HRP. For ApoD secretion, membranes were dyed with Amido Black as a loading reference; for ApoD expression, membranes were incubation with a mouse monoclonal anti-β-actin (1:5000, Sigma-Aldrich). Proteins were revealed with chemiluminescence (ECL, GE Healthcare, Quebec, Canada) using the Fusion FX7 (Vilber Lourmat, France) apparatus and software.

2.8. Statistical Analysis

Data are expressed as mean ± SEM, and analyzed using Prism 5.0 Software (GraphPad, La Jolla, CA, USA). Significant differences between groups were evaluated either by Student *t* test (2 groups) or two-way ANOVA followed by a Bonferroni post-test (3 or more groups), as detailed in the legends. Differences were considered significant at $p < 0.05$.

3. Results

3.1. Bone Status of ApoD-null and hApoD Transgenic Mice

Microcomputed tomography (microCT) analysis of femora from the three mouse strains revealed reduced bone volume in trabecular and cortical regions of *ApoD*-null females when compared to wt females (Tables 2 and 3). This parameter was exacerbated by aging, ranging from 18% in 3-month-olds to 50% 9-month-olds. Bone loss was associated to lower trabecular number and reduced trabecular thickness (Fig. 1A, top row and Table 2). Trabecular structure of *ApoD*-null males and h*ApoD*-tg mice of either gender remained unchanged. As shown in Table 3 and Fig. 1A (bottom row), cortical bone volumes were progressively reduced with age in both female and male *ApoD*-null mice, ranging from 13% at 3 months (non-significant) to 23% at 9 months. This parameter in *ApoD*-null mice was also 24% lower in all age groups when compared to gender-matched wt mice. Loss of cortical bone volume was associated to reduce cortical thickness and diameter for both male and female null mice.

Calcium and phosphorus plasma levels were measured in 9-month-old mice; no difference was noticed for either parameter between wt, tg and null mice (Table 4). Total plasma ALP levels were 120% higher in females relatively to males, independently of genotype; this parameter was augmented by 40% in *ApoD*-null females *versus* gender-matched wt mice. Histological analysis was performed on 9-month-old mice of all three genotypes; Von Kossa (VK) staining of mineralized bone area was reduced in femora sections from *ApoD*-null female mice compared to wt mice (Fig. 1B, top row; Table 4, not significant). Over 50% greater osteoblast surface was observed in bone tissue of females *versus* that of males, independently of genotype. This parameter was also 20% higher in null *versus* wt females (Fig. 1B, middle row; Table 4). In null females, this was accompanied by a 20% rise in osteoclast number (TRAP positive cells) (Fig. 1B, bottom row; Table 4); the null male bones also showed a 15% increase. No significant differences were noted in tg mouse femora through either microCT or histological analysis.

3.2. Impact of ApoD Deficiency or Supplementation on Osteoblast Differentiation

Since the low bone mass phenotype was more pronounced in female femora, *ApoD* expression was compared between MSC

Table 2 – Trabecular bone morphometric parameters in 3- to 9-month-old wt, *ApoD*-null and h*ApoD*-tg mice.

Gender	Age (months)	Genotype	Trabecular bone volume (%)	Number of trabeculae (mm^{-1})	Trabecular thickness (μm)
Male	3	wt	7.5 ± 0.9	1.75 ± 0.81	39.0 ± 2.4
		null	6.2 ± 1.5	1.70 ± 0.65	35.5 ± 2.9
		tg	6.8 ± 0.2	1.69 ± 0.41	36.8 ± 4.3
	6	wt	8.7 ± 0.4	2.09 ± 0.46	49.2 ± 6.7
		null	10.3 ± 1.7	2.40 ± 0.62	43.1 ± 1.5
		tg	6.8 ± 0.5	1.97 ± 0.26	47.9 ± 3.0
	9	wt	7.5 ± 1.4	1.79 ± 0.52	45.7 ± 3.7
		null	7.6 ± 1.8	1.60 ± 0.59	46.5 ± 7.6
		tg	6.7 ± 1.0	1.69 ± 0.43	45.1 ± 6.0
Female	3	wt	5.6 ± 1.0	1.51 ± 0.76	42.7 ± 4.2
		null	4.6 ± 0.1	1.23 ± 0.11	40.3 ± 5.3
		tg	5.7 ± 1.2	1.67 ± 0.54	46.3 ± 2.0
	6	wt	6.2 ± 1.1	1.63 ± 0.27	50.1 ± 7.1
		null	**3.2 ± 0.3**[a]	**0.80 ± 0.20**[a]	**36.5 ± 3.7**[c]
		tg	4.9 ± 0.8	1.73 ± 0.26	45.9 ± 0.2
	9	wt	6.4 ± 1.0	1.58 ± 0.84	45.7 ± 4.8
		null	**2.8 ± 0.4**[a]	**0.68 ± 0.12**[a]	**36.6 ± 6.6**[a]
		tg	4.4 ± 0.9	1.55 ± 0.40	50.1 ± 5.7

Femora were harvested from 4 to 8 (males) or 6–10 (females) mice per group and were analyzed as outlined in the materials and methods section. Values are mean ± SEM. Significant differences vs. age- and gender-matched wt: a = $p < 0.05$, c = $p < 0.001$, 2-way ANOVA followed by Bonferroni post-hoc test.

harvested from male and female wt mice. *ApoD* gene expression was found to be 1.5-fold higher in MSC isolated from females (Fig. 2A). In parallel, the *Rankl* to *Opg* mRNA ratio – an index of osteoclastogenesis [34] – was twice as high in *ApoD* null MSC derived from females (Fig. 2B); though this index was also elevated in male null MSC, it was not found to be significant. All further experiments were therefore carried out on MSC harvested from female marrow. *ApoD*-null MSC showed significantly reduced *in vitro* survival at day 14 (Fig. 2C), with a proliferation rate of 0.5-fold that of wt cells. These cells are also capable of internalizing exogenous hApoD (Fig. 2D); we therefore tested its effect on wt and null osteoblasts compared to basal and osteogenic media.

We first verified whether exogenous hApoD could influence the *Rankl*:*Opg* ratio; this treatment corrected the ratio back to wt cell control values (Fig. 3A). Because some studies associate higher serum *Rankl*:*Opg* ratio to oxidative stress [35], the expression of superoxide dismutase 1 (*Sod1*) was observed under the same conditions: *Sod1* expression paralleled the *Rankl*:*Opg* mRNA ratio (Fig. 3B), suggesting the involvement of

Table 3 – Cortical bone morphometric parameters in 3- to 9-month-old wt, *ApoD*-null and h*ApoD*-tg mice.

Gender	Age (months)	Genotype	Cortical bone volume (mm^3)	Cortical thickness (μm)	Cortical diameter (mm)
Male	3	wt	38.1 ± 1.2	132.5 ± 10.4	0.87 ± 0.08
		null	**28.4 ± 1.2**[b]	109.5 ± 8.6	0.82 ± 0.10
		tg	33.5 ± 2.5	141.8 ± 11.8	0.91 ± 0.08
	6	wt	41.8 ± 1.6	148.7 ± 2.0	1.17 ± 0.06
		null	**30.1 ± 0.6**[c]	**95.2 ± 9.6**[b]	**0.75 ± 0.08**[b]
		tg	49.6 ± 9.1	164.4 ± 5.4	1.14 ± 0.02
	9	wt	40.8 ± 1.1	142.1 ± 6.6	1.18 ± 0.05
		null	**32.8 ± 3.1**[a]	**103.3 ± 19.9**[a]	**0.82 ± 0.16**[a]
		tg	42.6 ± 5.6	127.7 ± 8.6	1.11 ± 0.05
Female	3	wt	36.0 ± 2.1	137.1 ± 8.1	1.18 ± 0.05
		null	31.2 ± 3.4	122.4 ± 24.6	1.19 ± 0.02
		tg	33.0 ± 2.3	131.5 ± 29.4	0.95 ± 0.06
	6	wt	43.5 ± 1.9	177.8 ± 7.2	1.48 ± 0.07
		null	**33.1 ± 1.1**[b]	**122.2 ± 15.4**[b]	**0.95 ± 0.09**[c]
		tg	52.1 ± 6.7	147.5 ± 19.5	1.17 ± 0.04
	9	wt	44.5 ± 4.4	183.0 ± 19.3	1.37 ± 0.14
		null	**34.1 ± 1.7**[a]	**122.1 ± 11.7**[a]	**0.99 ± 0.11**[a]
		tg	47.5 ± 5.2	173.6 ± 31.0	1.40 ± 0.12

Femora were harvested from 4 to 8 (males) or 6–10 (females) mice per group and were analyzed as outlined in the materials and methods section. Values are mean ± SEM. Significant differences vs. age- and gender-matched wt: a = $p < 0.05$, b = $p < 0.01$, c = $p < 0.001$, 2-way ANOVA followed by Bonferroni post-hoc test.

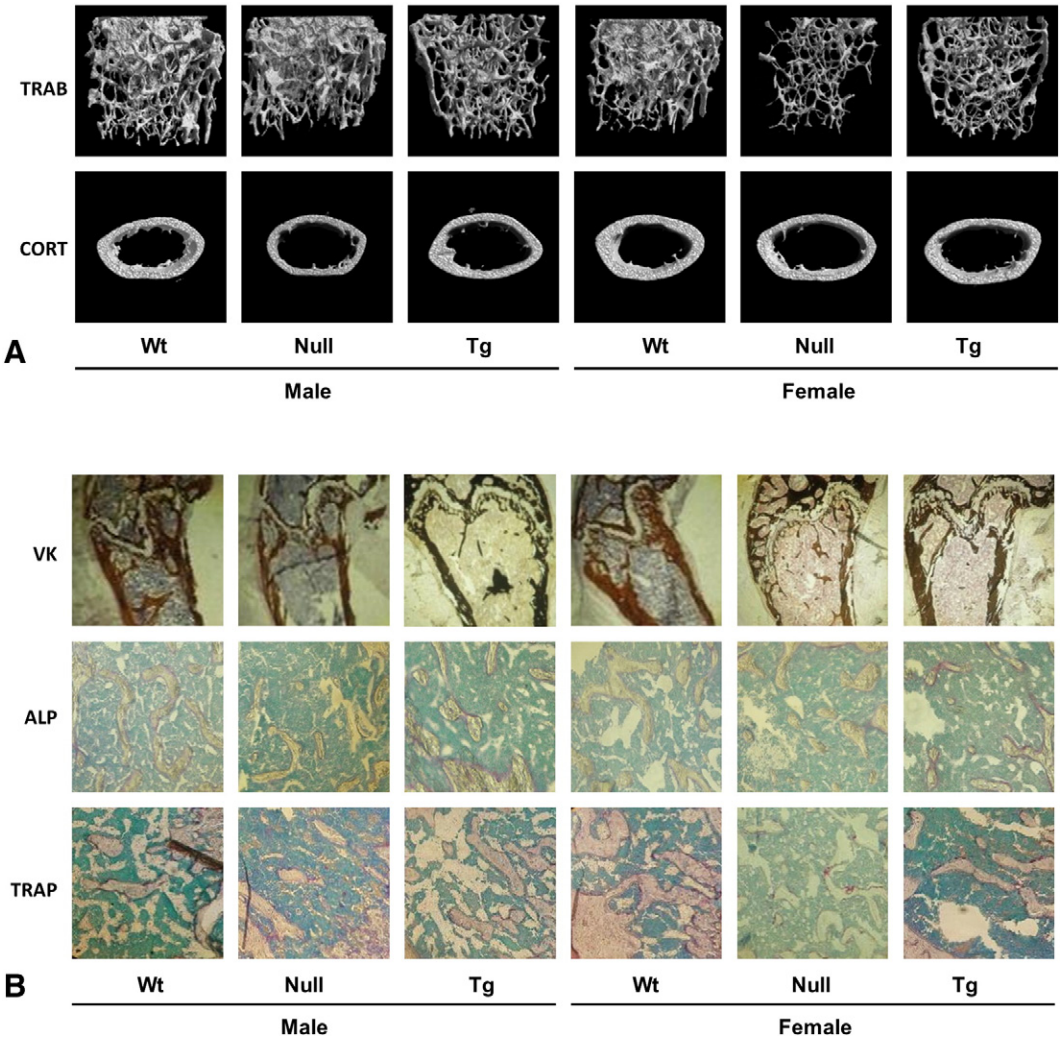

Fig. 1 – Histochemical and morphometric analyses of femora from wt, *ApoD*-null and h*ApoD*-tg mice. (A) Representative 3D reconstructions of femoral trabecular (top panels) and cortical (bottom panels) bone portions from 9-month-old wt, *ApoD*-null and h*ApoD*-tg mice. (B) Representative histological sections from 9-month-old wt, *ApoD*-null and h*ApoD*-tg mice. Low-temperature polymerizing MMA embedded bones were sectioned, deplastified and stained for Von Kossa (VK, 4× magnification, top panels), alkaline phosphatase (ALP, 10× magnification, middle panels) and tartrate-resistant acid phosphatase (TRAP, 10× magnification, bottom panels).

Table 4 – Plasmatic and static histology parameters in 9-month-old wt, *ApoD*-null and h*ApoD*-tg mice.

Gender	Male			Female		
Genotype	wt	null	tg	wt	null	tg
ALP (IU/L)	206 ± 21	253 ± 41	265 ± 37	**466 ± 19**[a]	**654 ± 39**[a,b]	**478 ± 13**[a]
Pi (mg/dL)	12.9 ± 0.8	13.9 ± 0.4	14.0 ± 0.4	13.0 ± 0.7	14.6 ± 0.4	13.5 ± 0.8
Ca (mg/dL)	9.7 ± 0.2	9.4 ± 0.3	9.5 ± 0.2	9.1 ± 0.2	9.6 ± 0.2	9.8 ± 0.2
Ca × Pi[1]	125 ± 10	131 ± 7	133 ± 6	117 ± 10	140 ± 6	132 ± 10
B.Ar/T.Ar (%)	15.1 ± 2.1	14.9 ± 1.4	15.3 ± 2.0	9.1 ± 0.8	5.6 ± 0.6[ns]	10.4 ± 0.6
Ob.S (%)	22.8 ± 1.6	26.3 ± 1.3	23.9 ± 2.0	**34.3 ± 0.6**[a]	**41.1 ± 1.5**[a,c]	**35.7 ± 0.7**[a]
Oc.N (mm^{-1})	4.7 ± 0.1	**5.4 ± 0.1**[b]	5.1 ± 0.1	**5.9 ± 0.2**[a]	**7.1 ± 0.3**[a,d]	5.5 ± 0.2

Blood was obtained from 4 to 6 mice per group and plasma was analyzed as outlined in the materials and methods section. Bones were harvested from 4 to 6 mice per group and embedded, sectioned and stained as outlined in the materials and methods section. Values are mean ± SEM. Significant difference vs. male (a = $p < 0.001$) and vs. gender-matched wt (b = $p < 0.05$, c = $p < 0.01$, d = 0.001), 2-way ANOVA followed by Bonferroni post-test. Ns, non significant.

[1] Ca × Pi indices were obtained by multiplying Ca and Pi means within each group, and their relative errors were added to obtain the absolute error of the product.

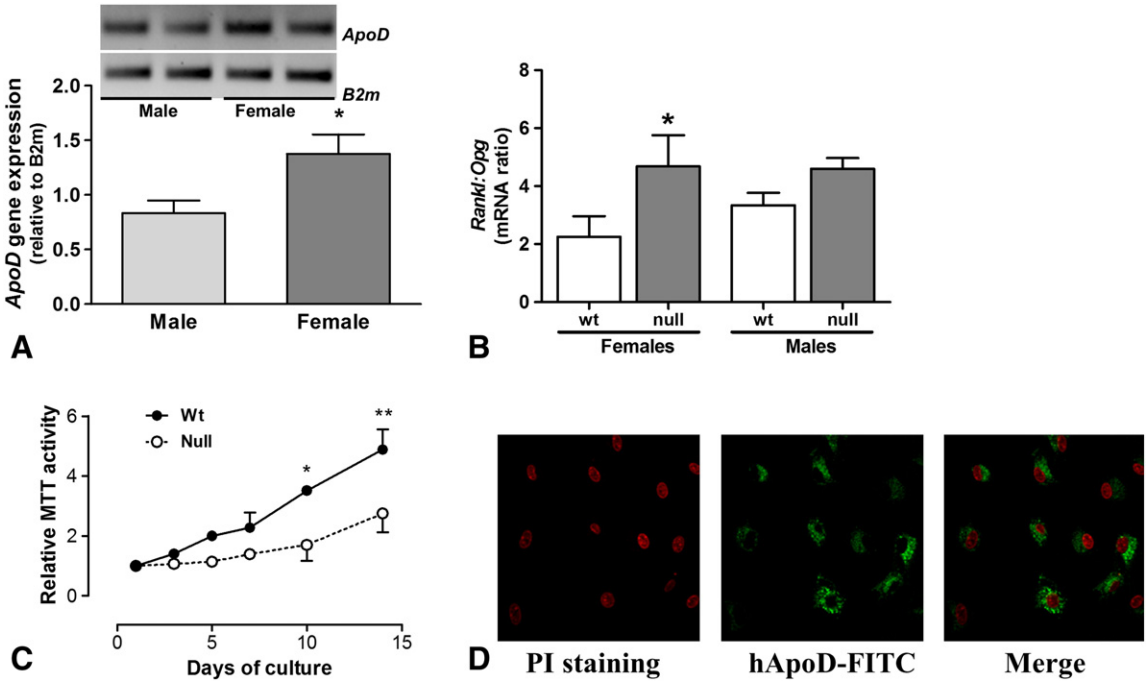

Fig. 2 – *ApoD* gene expression and uptake in MSC, and cell proliferation and *Rankl*:*Opg* ratio in wt and *ApoD*-null MSC. (A) Total RNA was isolated from MSC of male and female mice and real-time PCR was performed with specific primers for *ApoD* relative to expression levels of reference gene *B2m*. Values are the mean ± SEM of 4 independent cell preparations. Student *t* test (*p < 0.05) vs. male. Inset: representative PCR electrophoresis. (B) Real-time was performed with specific primers for *Opg* and *Rankl* to compare *Rankl*:*Opg* ratio in cells isolated from male and female wt or null mice. Values are the mean ± SEM of 3 independent experiments. Student *t* test (*p < 0.05) vs. gender-matched wt. (C) MSC from wt and *ApoD*-null female mice were seeded in 96-well plates and cultured for 14 days. MTT activity was measured to monitor the cell growth. Values are the mean ± SEM of 3 cell preparations. Bonferroni (*p < 0.05, **p < 0.01) vs. MTT activity for MSC from wt mice. (D) MSC from female wt mice were exposed to FITC-labeled hApoD and uptake was confirmed by confocal microscopy. Images are representative of 3 independent cell preparations.

oxidative stress in the anomalies observed in *ApoD*-null cells. An osteogenic treatment in mouse MSC was then performed for 14 days, since null MSC become difficult to maintain passed this time point. No difference was seen in basal ALP activity between wt and null MSC; however, null MSC did not respond to osteogenic treatment (Fig. 3C, left panel). Addition of hApoD showed an osteogenic effect on wt cells, and partially rescued the phenotype of null cells. Note that obtaining uniform monolayers of null cells was challenging in the untreated and osteogenic conditions; the presence of hApoD in the medium seemed to correct that situation (Fig. 3C, right panel).

To explore the relationship between ApoD and osteoblastic differentiation, we investigated its expression and secretion in differentiating MC3T3 cells, using a classical ascorbic acid and glycerol-2-phosphaste medium (Fig. 4A). As shown in Fig. 4B, *ApoD* gene expression was upregulated over 2-fold at 7 days of osteogenic treatment and onwards. In accordance, ApoD cellular protein levels were increased under these conditions (Fig. 4C, top panel), showing concomitant increase of ApoD secretion in culture medium (Fig. 4C, bottom panel). As was performed on MSC, ALP activity was monitored following 21 days in basal or osteogenic medium, or following addition of hApoD (Fig. 4D). hApoD alone also significantly enhance ALP activity in MC3T3 cells, although not being as potent as regular osteogenic medium.

3.3. *Influence of Growth Arrest on ApoD Gene Expression in MC3T3-E1 Cells*

Because ApoD deficiency seemed to impair MSC survival and confluence, we evaluated *ApoD* gene expression regulation in MC3T3 cells under various growth conditions. Given that growth arrest is associated with *ApoD* upregulation in fibroblasts and several other cell types [9,10], we observed its expression in serum-starved MC3T3 cells. As shown in Fig. 5A (left panel), serum starvation reduced by 15% the number of cells in S and G2/M phases, with a concurrent increase of cells in G1 phase. In accordance, BrdU incorporation was significantly reduced by serum deprivation (Fig. 5A, middle panel). Under these conditions, *ApoD* gene expression in MC3T3 cells was increased 1.5-fold (Fig. 5A, right panel). Given that MC3T3 cells are sensitive to contact inhibition, we verified *ApoD* gene expression in sub-confluent (70% of totalarea), confluent (100% of total area) and post-confluent (3 days after confluence) cell monolayers. As shown in Fig. 5B (left panel), cell percentage in the S and G2/M phases was significantly reduced by 16% to 26% in confluent and post-confluent monolayers, shifting cells to G1 phase with a concurrent reduction in DNA synthesis (Fig. 5B, middle panel). Under these culture conditions, *ApoD* gene expression was increased 1.42-fold (Fig. 5B, right panel).

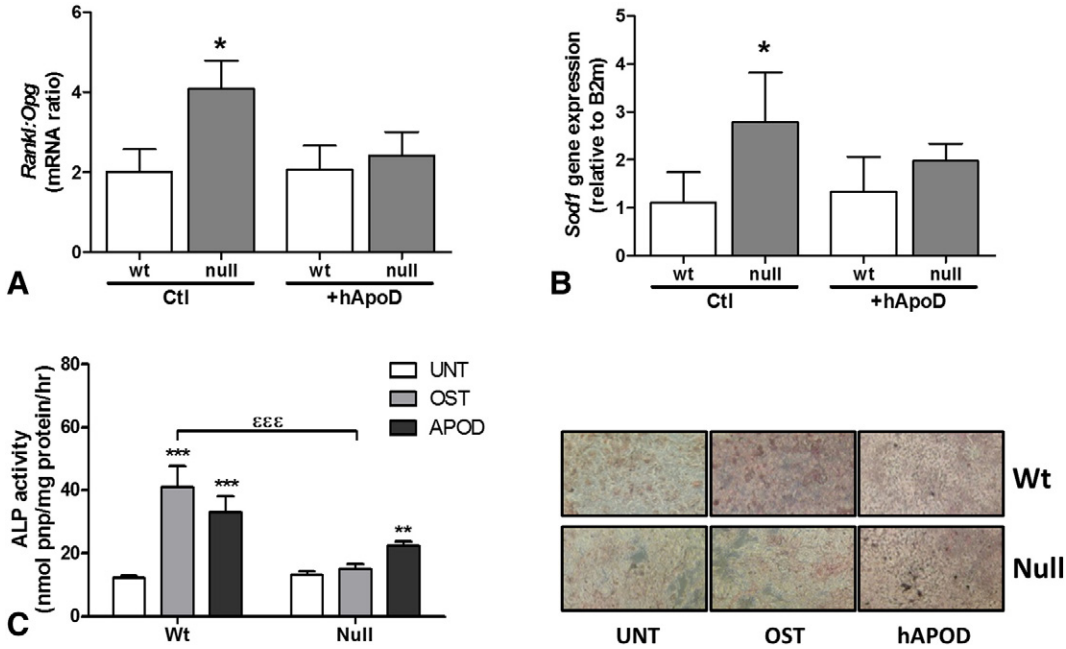

Fig. 3 – Impact of exogenous hApoD on *Rankl*:*Opg* ratio, *Sod1* expression and osteoblastic differentiation of wt and *ApoD*-null MSC. (A) *Rankl*:*Opg* ratio and (B) *Sod1* expression in female wt and null MSC with or without exogenous hApoD treatment. Values are the mean ± SEM of 3 independent experiments. Student t test (*p < 0.05) compared to untreated wt. (C) wt and *ApoD*-null MSC were cultured for 14 days in basal medium (UNT), osteogenic medium (OST) or with 250 ng/mL hApoD (APOD). ALP activity was evaluated through *p*-NPP conversion to *p*-NP and cytochemical staining. Values are the mean ± SEM of 3 cell preparations. Bonferroni (p < 0.01, ***p < 0001) vs. wt UNT and (εεεp < 0.001) vs. wt OST.**

4. Discussion

Osteoporosis is a health issue with significant morbidity and social cost [36]. This pathology is defined as lower bone mass and higher bone fragility [37]. Several risk factors have been identified that alter osteoblast and osteoclast activities; besides age, ethnicity and gender, numerous metabolic and genetic disorders translate to inadequate bone turnover [37,38]. The aim of the present study was to confirm the role of ApoD in osteoblastic cells and consequently, in proper bone turnover. Our results indicate that *ApoD* is upregulated in osteoblasts under conditions that reduce proliferation rate. Contact inhibition and osteogenic differentiation both upregulated *ApoD* gene expression; moreover, its addition to culture media enhances osteogenic differentiation to some extent, suggesting a paracrine contribution to this process. In accordance with its suggested role in osteoblast function, *ApoD*-null female mice display lower trabecular and cortical bone volumes with concurrent higher osteoblast surface and number of osteoclasts. Only cortical bone volume was reduced in *ApoD*-null male mice, arguing for gender-specific interactions.

The contribution of ApoD to bone metabolism *in vivo* was investigated by documenting bone status in *ApoD*-null and h*ApoD*-tg mice. Our results show that bone mass in null female mice was significantly reduced at both trabecular and cortical levels. Low bone volume in *ApoD*-null females was associated to reduced trabecular thickness and number of trabeculae particularly accentuated with age, hinting that ApoD may play a significant role in age-related bone loss. Histochemical analysis of 9-month-old mouse femora revealed greater relative osteoblast staining and higher number of TRAP-positive cells, suggesting accelerated bone turnover in null females. Mineral plasma homeostasis of 9-month-old null and tg mice was similar to that of wt mice; however, a significant increase in plasma ALP activity was noted in the null females only. Low bone mass accompanied by high serum ALP has been reported in cases of accelerated bone turnover in post-menopausal women [39]. This phenotype bears similarities with aged human bone, which commonly shows reduced wall thickness in histological sections, an index of reduced bone matrix deposition. This condition may be associated to an increased activation frequency of bone remodeling units [40].

In contrast, only the femoral cortex was altered in *ApoD*-null male mice. Higher *ApoD* gene expression was measured in MSC from females compared to those from male mice, suggesting that ApoD contributes to a higher extent in female bone metabolism, at least as age progresses. In accordance, higher *ApoD* expression levels in the CNS are also measured in women, and increase with aging in women but not in men [37]. The link between the gender-specific bone effects of ApoD and sex steroids remains unclear. The *ApoD* promoter shows estrogen response elements and thus, its expression and secretion could be influenced by sex steroids in breast cyst fluid [9,41] and breast cancer cells [20,42]. Other gender-specific effects have been reported; for instance, the neuroprotective effect of ApoD against human coronavirus OC43-induced encephalitis is greater in male mice, as they are more sensitive to this infection [43]. Perhaps the ability of ApoD to bind progesterone and

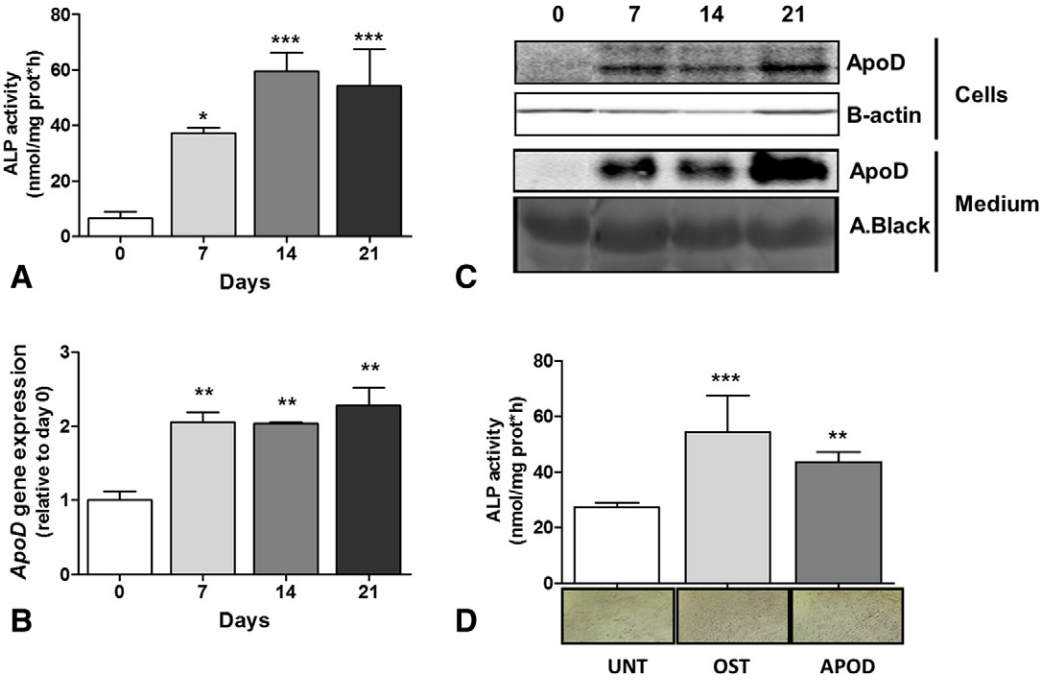

Fig. 4 – *ApoD* expression in differentiated murine MC3T3 cells. (A-B-C) MC3T3 cells were cultured in osteogenic media for 7, 14 and 21 days. (A) ALP activity was monitored through *p*-NPP conversion to *p*-NP and cytochemical staining. (B) *ApoD* gene expression was determined by real-time PCR relative to basal expression (day 0, i.e. confluence). (A-B) Values are mean ± SEM of 3 cell passages. Bonferroni (*p < 0.05, **p < 0.01, ***p < 0.001) vs. day 0. (C) Cell lysates (upper panels) and culture media (bottom panels) were collected at the end of treatments and ApoD protein levels were determined by immunoblotting. Pictures are representative of 3 cell passages. (D) MC3T3 cells were cultured for 21 days in regular medium (UNT) with or without hApoD (APOD) or osteogenic media (OST) and ALP was evaluated through p-NPP conversion to p-NP and cytochemical staining. Data are representative of 3 cell passages. Student t test (p < 0.01, ***p < 0.001) vs. UNT.**

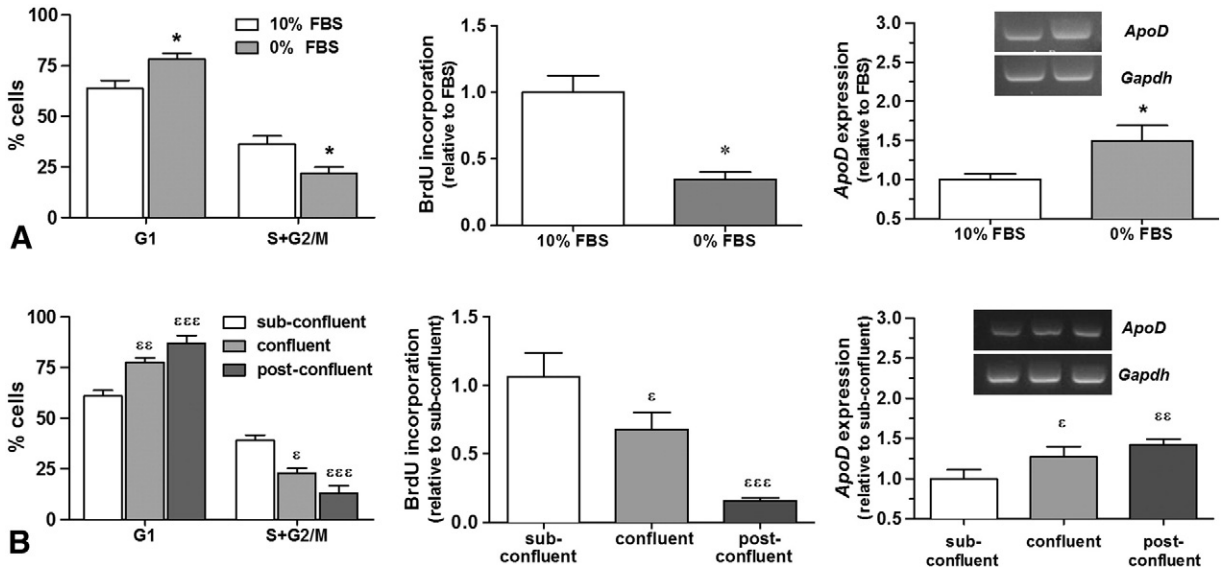

Fig. 5 – Reduced cell proliferation enhances *ApoD* gene expression in MC3T3 cells. Cells were cultured (A) for 48 h in medium with or without 10% FBS, or (B) cultured in medium containing 10% FBS until the monolayer reaches 70% confluence (sub-confluent), 100% confluence and 3 days after the confluence (post-confluent). Cells were labeled with PI for cell cycle analysis by flux cytometer (left panels), used for BrdU incorporation to measure DNA synthesis (middle panels) or for total RNA isolation to determine the relative levels of *ApoD* gene expression by RT-PCR (right panels; inset-representative PCR products electrophoresis). Values are expressed as mean ± SEM of 3 to 8 cell passages. Student t test (*p < 0.05) vs. condition with FBS; Bonferroni (εp < 0.05, εεp < 0.01, εεεp < 0.001) vs. sub-confluent condition.

pregnenolone might explain some of the gender-related differences. Since *ApoD* deletion predominantly impacts bone in aged female mice, ovariectomy-induced bone loss in this model could discriminate between ApoD-dependant and hormone-dependant effects.

ApoD-null MSC were found to have significantly impaired proliferation and differentiation. These data corroborate the idea of accelerated bone turnover, as reduced osteoblastic life span due to microenvironmental stress has been associated to accelerated remodeling [44]. We observed enhanced *ApoD* gene expression in MC3T3 cells under osteogenic culture conditions. This result agrees with the reported *ApoD* upregulation with osteogenic differentiation of human MSC [28] and mouse primary osteoblasts [30], as well as high-throughput gene expression profile (biogps.org, ID11815) and microarray analyses of C3H10 cells [29]. Moreover, we report that osteogenic differentiation is associated with increased cellular and secreted ApoD protein levels in MC3T3 cells, arguing for an auto/paracrine function of ApoD in bone metabolism. Mouse MSC readily uptake the protein from media; accordingly, treatment with exogenous hApoD increased ALP activity in undifferentiated MC3T3 cells, and partially rescued the osteogenic potential of *ApoD*-null MSC.

The purpose for enhanced *ApoD* expression during osteogenic differentiation is unknown, but evidence suggests its requirement for osteoblast maturation and function. Robust energetic demands are placed on mature osteoblasts for matrix secretion and mineralization. In accordance, cellular respiration and mitochondrial activities are increased, likely maintaining higher ATP levels observed in mature osteoblast [45]. Accordingly, antioxidant enzymes manganese-dependent superoxide dismutase (SOD) and catalase were shown to be upregulated in human MSC upon osteogenic differentiation, likely to prevent the accumulation of intracellular ROS. Of note, there is increasing evidence for a prominent neuroprotective role of ApoD because of its antioxidant activity (reviewed in Ref. [46]). Loss of ApoD function increases, whereas ApoD overexpression reduces sensitivity to oxidative stress, as well as lipid peroxidation in brain tissue after oxidant treatment in mice [12]. Specifically, hApoD has been shown to reduce arachidonic acid hydroperoxides to lipid hydroxides, thus acting as a lipid antioxidant and preventing lipid peroxidation [47]. Therefore, *ApoD* upregulation during osteogenic differentiation may act as a protection mechanism against oxidative stress. Interestingly, the higher *Rankl*:*Opg* ratio and *Sod1* expression observed in female-derived null MSC were both rescued by exogenous hApoD, reinforcing the hypothesis of an antioxidant role of ApoD in bone tissue.

Oxidative stress was shown to decrease osteoblast life span as evidenced in osteoblasts from *Sod1*-null mice while preventing proper osteoclastogenesis, leading to low-turnover bone loss [48]; *ApoD*-null mice on the contrary display signs of high-turnover bone loss. Perhaps the impact of oxidative stress on bone remodeling is biphasic, with low or intermediate levels accelerating bone turnover while high levels impair it altogether. In addition, ApoD may also influence RANKL expression and activation through inflammatory pathways in bone microenvironment. By binding to arachidonic acid, its main ligand, ApoD may restrain its availability. Arachidonic acid is the major precursor of leukotrienes and prostaglandins, two groups of potent inflammatory modulators known to impact bone metabolism [52]. Oxidative stress is known to enhance osteoclastogenesis and inhibit osteoblastogenesis through NF-κB-mediated RANKL regulation [35,49]. It would be of interest to compare the levels of ROS and antioxidant components, as well as *Rankl*:*Opg* ratio between *ApoD*-null and *Sod1*-null MSC. Evidence from pharmacological and genetic studies in mice has provided support for a deleterious effect of oxidative stress in bone and has strengthened the idea that increased ROS levels with age represent a pathophysiological mechanism underlying age-related bone loss (reviewed in Ref. [50]).

Because increased *ApoD* gene expression occurs in several cell models following growth arrest and cell differentiation [9,42,51], we investigated *ApoD* gene expression in osteoblasts with regards to cell density. Low proliferation rate induced by serum starvation, as well as contact inhibition caused by confluence, both enhanced *ApoD* gene expression in MC3T3 cells. These conditions were associated with reduced BrdU incorporation and lower proportion of cells in the S and G2/M phases, confirming proliferation arrest. Similar *ApoD* upregulation by growth arrest was observed in human and murine fibroblasts, as well as in various cancer cell lines [9,10,11,51]. Alternating purine pyrimidine (APP) stretches and serum response elements (SRE) in the promoter of h*ApoD* gene were found to significantly contribute to growth arrest-induced *ApoD* gene expression [9]. Further mechanistic studies revealed the importance of Parp-1, APEX-1 and ERK1 catalytic activities in the growth arrest-induced *ApoD* gene expression [51].

5. Conclusions

In light of the present data, we suggest that ApoD deficiency causes high bone turnover by impairing osteoblast life span and differentiation. Considering ApoD's property to limit oxidative stress [12,45,46], it may interact with key processes in osteoblasts. ApoD might not only bind and transport lipophilic molecules, but may also actively interfere with their metabolism and signaling in an antioxidant and anti-inflammatory manner.

Overall, our results indicate that ApoD contributes to the regulation of bone metabolism in mice and further studies are required to pinpoint its mechanisms. The evidence of ApoD secretion and uptake by osteoblasts suggest a paracrine function, potentially representing a novel marker of age-related bone loss.

Author Contributions

RM and ER designed the study; CM, ON and CS conducted the study, collected and analyzed the data; CM, ON, CS, RM and ER interpreted the data; RM, CM, ON and CS drafted the manuscript; CM, ON, CS and ER revised and approved the final version.

Grants

This work was supported by the Canadian Institutes of Health Research grants MOP-37994 (ER) and MOP-89958 (RM) and a catalyst grant to both ER and RM.

Disclosures

No conflicts of interest, financial or otherwise, are declared by the authors.

Acknowledgments

We thank Denis Flipo for his help with the confocal microscopy analysis. Special thanks to Robert Moreau for investing time and energy in spite of his illness.

REFERENCES

[1] Eriksen EF. Cellular mechanisms of bone remodeling. Rev Endocr Metab Disord 2010;11:219–27.
[2] Lian JB, Stein GS, Javed A, van Wijnen AJ, Stein JL, Montecino M, et al. Networks and hubs for the transcriptional control of osteoblastogenesis. Rev Endocr Metab Disord 2006;7:1–16.
[3] Raisz LG. Pathogenesis of osteoporosis: concepts, conflicts, and prospects. J Clin Invest 2005;115:3318–25.
[4] McConathy WJ, Alaupovic P. Isolation and partial characterization of apolipoprotein D: a new protein moiety of the human plasma lipoprotein system. FEBS Lett 1973; 37:178–82.
[5] Seguin D, Desforges M, Rassart E. Molecular characterization and differential mRNA tissue distribution of mouse apolipoprotein D. Brain Res Mol Brain Res 1995;30:242–50.
[6] Drayna D, Fielding C, McLean J, Baer B, Castro G, Chen E, et al. Cloning and expression of human apolipoprotein D cDNA. J Biol Chem 1986;261:16535–9.
[7] Rassart E, Bedirian A, Do Carmo S, Guinard O, Sirois J, Terrisse L, et al. Apolipoprotein D. Biochim Biophys Acta 2000;1482: 185–98.
[8] Vogt M, Skerra A. Bacterially produced apolipoprotein D binds progesterone and arachidonic acid, but not bilirubin or E-3M2H. J Mol Recognit 2001;14:79–86.
[9] Do Carmo S, Seguin D, Milne R, Rassart E. Modulation of apolipoprotein D and apolipoprotein E mRNA expression by growth arrest and identification of key elements in the promoter. J Biol Chem 2002;277:5514–23.
[10] Provost PR, Marcel YL, Milne RW, Weech PK, Rassart E. Apolipoprotein D transcription occurs specifically in nonproliferating quiescent and senescent fibroblast cultures. FEBS Lett 1991;290:139–41.
[11] Do Carmo S, Levros Jr LC, Rassart E. Modulation of apolipoprotein D expression and translocation under specific stress conditions. Biochim Biophys Acta 2007;1773:954–69.
[12] Ganfornina MD, Do Carmo S, Lora JM, Torres-Schumann S, Vogel M, Allhorn M, et al. Apolipoprotein D is involved in the mechanisms regulating protection from oxidative stress. Aging Cell 2008;7:506–15.
[13] Goodrum JF, Earnhardt T, Goines N, Bouldin TW. Fate of myelin lipids during degeneration and regeneration of peripheral nerve: an autoradiographic study. J Neurosci 1994; 14:357–67.
[14] Spreyer P, Schaal H, Kuhn G, Rothe T, Unterbeck A, Olek K, et al. Regeneration-associated high level expression of apolipoprotein D mRNA in endoneurial fibroblasts of peripheral nerve. EMBO J 1990;9:2479–84.
[15] Terrisse L, Seguin D, Bertrand P, Poirier J, Milne R, Rassart E. Modulation of apolipoprotein D and apolipoprotein E expression in rat hippocampus after entorhinal cortex lesion. Brain Res Mol Brain Res 1999;70:26–35.
[16] Thomas EA, Dean B, Pavey G, Sutcliffe JG. Increased CNS levels of apolipoprotein D in schizophrenic and bipolar subjects: implications for the pathophysiology of psychiatric disorders. Proc Natl Acad Sci U S A 2001;98:4066–71.
[17] Van Dijk W, Do Carmo S, Rassart E, Dahlbäck B, Sodetz J. The plasma lipocalins alpha1-acid glycoprotein, apolipoprotein D, apolipoprotein M and complement protein C8gamma. In: Akerström B, Borregaard N, Flower DR, Salier J-P, editors. Lipocalins, Landes bioscience; 2006. p. 140–66.
[18] Ordonez C, Navarro A, Perez C, Martinez E, del Valle E, Tolivia J. Gender differences in apolipoprotein D expression during aging and in Alzheimer disease. Neurobiol Aging 2012;33: 433.e11-e20.
[19] Alvarez ML, Barbon JJ, Gonzalez LO, Abelairas J, Boto A, Vizoso FJ. Apolipoprotein D expression in retinoblastoma. Ophthalmic Res 2003;35:111–6.
[20] Simard J, de Launoit Y, Haagensen DE, Labrie F. Additive stimulatory action of glucocorticoids and androgens on basal and estrogen-repressed apolipoprotein-D messenger ribonucleic acid levels and secretion in human breast cancer cells. Endocrinology 1992;130:1115–21.
[21] Alaupovic P, Schaefer EJ, McConathy WJ, Fesmire JD, Brewer Jr HB. Plasma apolipoprotein concentrations in familial apolipoprotein A-I and A-II deficiency (Tangier disease). Metabolism 1981;30:805–9.
[22] Breckenridge WC, Little JA, Alaupovic P, Wang CS, Kuksis A, Kakis G, et al. Lipoprotein abnormalities associated with a familial deficiency of hepatic lipase. Atherosclerosis 1982;45: 161–79.
[23] Lane DM, McConathy WJ. Factors affecting the lipid and apolipoprotein levels of cord sera. Pediatr Res 1983;17:83–91.
[24] Alaupovic P, McConathy WJ, Curry MD, Magnani HN, Torsvik H, Berg K, et al. Apolipoproteins and lipoprotein families in familial lecithin: cholesterol acyltransferase deficiency. Scand J Clin Lab Invest Suppl 1974;137:83–7.
[25] Alaupovic P, Fernandes J. The serum apolipoprotein profile of patients with glucose-6-phosphatase deficiency. Pediatr Res 1985;19:380–4.
[26] Baker WA, Hitman GA, Hawrami K, McCarthy MI, Riikonen A, Tuomilehto-Wolf E, et al. Apolipoprotein D gene polymorphism: a new genetic marker for type 2 diabetic subjects in Nauru and South India. Diabet Med 1994;11:947–52.
[27] Vijayaraghavan S, Hitman GA, Kopelman PG. Apolipoprotein-D polymorphism: a genetic marker for obesity and hyperinsulinemia. J Clin Endocrinol Metab 1994;79:568–70.
[28] Ishii M, Koike C, Igarashi A, Yamanaka K, Pan H, Higashi Y, et al. Molecular markers distinguish bone marrow mesenchymal stem cells from fibroblasts. Biochem Biophys Res Commun 2005;332:297–303.
[29] Beak JY, Kang HS, Kim YS, Jetten AM. Kruppel-like zinc finger protein Glis3 promotes osteoblast differentiation by regulating FGF18 expression. J Bone Miner Res 2007;22:1234–44.
[30] Schilling AF, Schinke T, Munch C, Gebauer M, Niemeier A, Priemel M, et al. Increased bone formation in mice lacking apolipoprotein E. J Bone Miner Res 2005;20:274–82.
[31] Erben RG. Embedding of bone samples in methylmethacrylate: an improved method suitable for bone histomorphometry, histochemistry, and immunohistochemistry. J Histochem Cytochem 1997;45:307–13.
[32] Peterson WJ, Tachiki KH, Yamaguchi DT. Serial passage of MC3T3-E1 cells down-regulates proliferation during osteogenesis in vitro. Cell Prolif 2004;37:325–36.
[33] Moreau R, Aubin R, Lapointe JY, Lajeunesse D. Pharmacological and biochemical evidence for the regulation of osteocalcin secretion by potassium channels in human osteoblast-like MG-63 cells. J Bone Miner Res 1997;12:1984–92.
[34] Thomas GP, Baker SU, Eisman JA, Gardiner EM. Changing RANKL/OPG mRNA expression in differentiating murine primary osteoblasts. J Endocrinol 2001;170(2):451–60.

[35] Baek KH, Oh KW, Lee WY, Lee SS, Kim MK, Kwon HS, et al. Association of oxidative stress with postmenopausal osteoporosis and the effects of hydrogen peroxide on osteoclast formation in human bone marrow cell cultures. Calcif Tissue Int 2010;87(3):226–35.
[36] Weston JM, Norris EV, Clark EM. The invisible disease: making sense of an osteoporosis diagnosis in older age. Qual Health Res 2011;21:1692–704.
[37] Sandhu SK, Hampson G. The pathogenesis, diagnosis, investigation and management of osteoporosis. J Clin Pathol 2011;64:1042–50.
[38] O'Neill TW. Looking back: developments in our understanding of the occurrence, aetiology and prognosis of osteoporosis over the last 50 years. Rheumatology (Oxford) 2005(44 Suppl. 4): iv33–5.
[39] Mukaiyama K, Kamimura M, Uchiyama S, Ikegami S, Nakamura Y, Kato H. Elevation of serum alkaline phosphatase (ALP) level in postmenopausal women is caused by high bone turnover. Aging Clin Exp Res 2015;27:413–8.
[40] Garnero P, Sornay-Rendu E, Chapuy MC, Delmas PD. Increased bone turnover in late postmenopausal women is a major determinant of osteoporosis. J Bone Miner Res 1996;11(3): 337–49.
[41] Lambert J, Provost PR, Marcel YL, Rassart E. Structure of the human apolipoprotein D gene promoter region. Biochim Biophys Acta 1993;1172:190–2.
[42] Lopez-Boado YS, Tolivia J, Lopez-Otin C. Apolipoprotein D gene induction by retinoic acid is concomitant with growth arrest and cell differentiation in human breast cancer cells. J Biol Chem 1994;269:26871–8.
[43] Do Carmo S, Jacomy H, Talbot PJ, Rassart E. Neuroprotective effect of apolipoprotein D against human coronavirus OC43-induced encephalitis in mice. J Neurosci 2008;28:10330–8.
[44] Ng AH, Baht GS, Alman BA, Grynpas MD. Bone marrow stress decreases osteogenic progenitors. Calcif Tissue Int 2015;97: 476–86.
[45] Komarova SV, Ataullakhanov FI, Globus RK. Bioenergetics and mitochondrial transmembrane potential during differentiation of cultured osteoblasts. Am J Physiol Cell Physiol 2000;279: C1220–9.
[46] Dassati S, Waldner A, Schweigreiter R. Apolipoprotein D takes center stage in the stress response of the aging and degenerative brain. Neurobiol Aging 2014;35:1632–42.
[47] Bhatia S, Knoch B, Wong J, Kim WS, Else PL, Oakley AJ, et al. Selective reduction of hydroperoxyeicosatetraenoic acids to their hydroxy derivatives by apolipoprotein D: implications for lipid antioxidant activity and Alzheimer's disease. Biochem J 2012;442:713–21.
[48] Nojiri H, Saita Y, Morikawa D, Kobayashi K, Tsuda C, Miyazaki T, et al. Cytoplasmic superoxide causes bone fragility owing to low-turnover osteoporosis and impaired collagen cross-linking. J Bone Miner Res 2011;26:2682–94.
[49] Bai XC, Lu D, Bai J, Zheng H, Ke ZY, Li XM, et al. Oxidative stress inhibits osteoblastic differentiation of bone cells by ERK and NF-kappaB. Biochem Biophys Res Commun 2004; 314(1):197–207.
[50] Almeida M, O'Brien CM. Basic biology of skeletal aging: role of stress response pathways. J Gerontol A Biol Sci Med Sci 2013; 68(10):1197–208.
[51] Levros Jr LC, Do Carmo S, Edouard E, Legault P, Charfi C, Rassart E. Characterization of nuclear factors modulating the apolipoprotein D promoter during growth arrest: implication of PARP-1, APEX-1 and ERK1/2 catalytic activities. Biochim Biophys Acta 2010;1803:1062–71.
[52] Ren W, Dziak R. Effects of leukotrienes on osteoblastic cell proliferation. Calcif Tissue Int 1991;49:197–201.